

Contents lists available at ScienceDirect

Journal of Hydrology

journal homepage: www.elsevier.com/locate/jhydrol



Research papers

Drought monitoring with soil moisture active passive (SMAP) measurements



Ashok Mishra a,*, Tue Vu a, Anoop Valiya Veettil a, Dara Entekhabi b

- ^a Glenn Department of Civil Engineering, Clemson University, Clemson, SC 29634-0911, USA
- ^b Department of Civil and Environmental Engineering, Massachusetts Institute of Technology, Cambridge, MA, USA

ARTICLE INFO

Article history: Received 27 March 2017 Received in revised form 12 July 2017 Accepted 14 July 2017 Available online 18 July 2017

Keywords: Droughts SMAP SWDI AWD

ABSTRACT

Recent launch of space-borne systems to estimate surface soil moisture may expand the capability to map soil moisture deficit and drought with global coverage. In this study, we use Soil Moisture Active Passive (SMAP) soil moisture geophysical retrieval products from passive L-band radiometer to evaluate its applicability to forming agricultural drought indices. Agricultural drought is quantified using the Soil Water Deficit Index (SWDI) based on SMAP and soil properties (field capacity and available water content) information. The soil properties are computed using pedo-transfer function with soil characteristics derived from Harmonized World Soil Database. The SMAP soil moisture product needs to be rescaled to be compatible with the soil parameters derived from the in situ stations. In most locations, the rescaled SMAP information captured the dynamics of in situ soil moisture well and shows the expected lag between accumulations of precipitation and delayed increased in surface soil moisture. However, the SMAP soil moisture itself does not reveal the drought information. Therefore, the SMAP based SWDI (SMAP_SWDI) was computed to improve agriculture drought monitoring by using the latest soil moisture retrieval satellite technology. The formulation of SWDI does not depend on longer data and it will overcome the limited (short) length of SMAP data for agricultural drought studies. The SMAP_SWDI is further compared with in situ Atmospheric Water Deficit (AWD) Index. The comparison shows close agreement between SMAP_SWDI and AWD in drought monitoring over Contiguous United States (CONUS), especially in terms of drought characteristics. The SMAP_SWDI was used to construct drought maps for CONUS and compared with well-known drought indices, such as, AWD, Palmer Z-Index, sc-PDSI and SPEI. Overall the SMAP_SWDI is an effective agricultural drought indicator and it provides continuity and introduces new spatial mapping capability for drought monitoring. As an agricultural drought index, SMAP_SWDI has potential to capture short term moisture information similar to AWD and related drought indices.

© 2017 Elsevier B.V. All rights reserved.

1. Introduction

Soil moisture links water, energy and carbon cycles over land. Therefore, accurate estimation of soil moisture is critical and a precursor to formulate better water and land use management practices and hazards mitigation strategies (Brown et al., 2013). To date, there have been several satellites that provide soil moisture information with various degrees of accuracy, spatial resolution and temporal sampling such as Meteorological Operational Satellites (MetOp) which carrying Advanced SCATterometer (ASCAT) and NASA's Aqua which hosts the Advanced Microwave Scanning Radiometer for Earth Observing System (AMSR-E). In November 2009, the European Space Agency (ESA) launched the satellite mis-

* Corresponding author.

E-mail address: ashokm@g.clemson.edu (A. Mishra).

sion: the Soil Moisture and Ocean Salinity (SMOS), which being the first mission specifically dedicated to Earth's surface soil moisture (Kerr et al., 2010). The SMOS carries an aperture synthesis L-band radiometer (1.41 GHz) for the estimation of surface parameters at an approximately 40 km resolution which provide estimates of surface soil moisture within approximately the top 5 cm. Since launched, numerous studies have utilized the SMOS soil moisture datasets for many applications such as deriving drought index (Martínez-Fernández et al., 2016; Scaini et al., 2015), quantifying drought impacts on crop yield (Chakrabarti et al., 2014) or hydro-meteorological application (Zhuo et al., 2015). There have been a number of comparisons between these satellites' soil moisture product with in situ datasets (Brocca et al., 2011; Parrens et al., 2012; Fascetti et al., 2016).

Recently, Soil Moisture Active Passive (SMAP; Entekhabi et al., 2010a) satellite was launched by NASA (in January 2015) to map

surface soil moisture information from space. SMAP carries sensors of an active L-band radar 3 km (1.26 GHz) and a passive L-band radiometer 36 km (1.41 GHz) on a single platform and to provide a combined global measurement of surface soil moisture at an intermediate spatial resolution of 9 km (Entekhabi et al., 2010a, 2015). SMAP will compliment a host of passive and active sensors including the SMOS mission, AMSR2, RADARSAT-2, Sentinel-1, TerraSAR-X, COSMO-SkyMed and ALOS-2 (McNairn et al., 2015). Unfortunately, the SMAP 3 km active L-band radar failed after two months in orbit but the 36 km radiometer continues to produce information that is valuable to constrain land surface models in data assimilation.

Although surface soil moisture data obtained from different sources (e.g., satellite retrievals and land surface models) have been shown to contain consistent and useful information in their seasonal cycle and anomaly signals, they typically exhibit very different mean values and variability. Often bias removal is necessary in order to compare the diagnostics formed based on each data source (Reichle and Koster, 2004). Cumulative Distribution Function (CDF) matching technique has been widely used for correcting satellite based soil moisture biases (Reichle and Koster, 2004; Draper et al., 2009). These techniques are aimed at re-scaling two data sets that have consistent averages and/or consistent dynamic ranges. Therefore, in this study, we apply CDF matching approach to remove the systematic bias and dynamic range differences between SMAP soil moisture and in situ datasets.

The advancement made in satellite based soil moisture measurement can add new capability for agricultural drought monitoring. Agricultural drought refers to a period with declining soil moisture and consequent crop failure without any reference to surface water resources (Mishra and Singh, 2010). Satellite data are applied for drought studies (Martínez-Fernández et al., 2016; Hao and AghaKouchak, 2013; Ahmadalipour et al., 2016; Anderson et al., 2013; Crow et al., 2012; Sheffield and Wood, 2008; Bartalis et al., 2007) as well as to investigate local-scale agricultural drought anatomy (Mishra et al., 2015). Shellito et al. (2016) suggested SMAP soil moisture drying is more rapid than in situ following rainfall events. The applications of SMAP for agricultural drought studies are very limited due to the unavailability of SMAP data for longer time period. To overcome this limitation we use SWDI as an agriculture drought index that is derived based on the soil water characteristics (i.e., Field capacity and Available water content). The SWDI was selected in this study because its formulation does not depend on longer data unlike other standardized drought indices (e.g., Standardized Precipitation Index, Standardized Soil Moisture Index, etc.) derived based on the anomalies of long term data sets. Therefore selection of SWDI will overcome the limited (short) length of SMAP data for agricultural drought studies.

The main objectives of this paper are twofold: 1) Produce SMAP-based agricultural drought indices (SMAP_SWDI) for Contiguous United States (CONUS), where in situ soil moisture records are available for comparison and evaluation, and 2) Compare SMAP_SWDI with other agriculture drought index (i.e., Atmospheric Water Deficit index) derived from precipitation and temperature data as inputs. Section 2 describes the in situ and SMAP satellite data products. Section 3 presents the methodology used for re-scaling and introduces drought indices. Section 4 provides results. Discussions and conclusions are drawn in Section 5.

2. Data

2.1. In situ datasets

The US Climate Reference Network (USCRN; https://www.ncdc.noaa.gov/crn/) operated by the National Oceanic and Atmospheric

Administration (NOAA) provides high-quality long term temperature, precipitation, soil moisture and soil temperature observations. The USCRN stations are installed over CONUS using triplicate-configuration soil moisture and soil temperature probes at five standard depths (5 cm, 10 cm, 20 cm, 50 cm and 100 cm) (Bell et al., 2013). USCRN has also been used for the validation program of SMAP but not within the Core Validation Sites (Jackson et al., 2012; Pan et al., 2016; Velpuri et al., 2016). Detailed information related to USCRN can be found in Diamond et al. (2013) and Bell et al. (2013). Using USCRN database, we selected 104 stations that are spatially distributed across CONUS and have one full year data length from 1st April 2015 to 31st March 2016. The criteria for selecting 104 stations are based on the availability of in situ and SMAP pixel for the entire study period.

2.2. SMAP L3 soil moisture information

The SMAP satellite mission was launched by NASA in January 2015 (Entekhabi et al., 2010a) to retrieve global soil moisture information via measuring brightness temperature through geophysical inversion. Different levels of SMAP products are defined as Level 2 for half orbit based, Level 3 for daily composites and Level 4 for model assimilation (Brown et al., 2013). Lying in the midlatitudes where the neighboring swaths do not overlap, Level 2 and Level 3 are essentially no difference (Pan et al., 2016). In conjunction with a forward model of brightness temperature and ancillary products, the SMAP L3 is an estimate of surface soil moisture within the top 5 cm of the soil column (O'Neill et al., 2016). There are tentatively three products of SMAP L3 soil moisture that can be collected from National Snow and Ice Data Center (NSIDC): (1) The passive L-band radiometer 36 km (1.41 GHz) (2) The active L-band radar 3 km (1.26 GHz) and (3) The combined active/passive L-band product at 9 km (Entekhabi et al., 2015). However, we only choose the passive L-band radiometer 36 km resolution product for drought analysis in this study, because of the failure of the active Lband radar 3 km after two months in orbit. The detailed information on how SMAP L3 Passive data (SM_L3_P) is retrieved, processed can be found in O'Neil et al. (2015). Over CONUS, SMAP was calibrated and validated for eight in situ in the Core Validation Sites (CVS) with objective to reduce the unbiased root mean square error below 0.04 m³/m³ (Jackson et al., 2016).

Bilinear interpolation approach was used to estimate the satellite soil moisture information at in situ locations based on four adjacent grid points. This method ensures that the closest grid point to the station will be given the highest weight. This similar interpolation technique was used to extract even more spatially variable co-located station rainfall data from satellite precipitation (Vu et al., 2012, 2015; Rozante et al., 2010).

3. Methodology

3.1. Rescaling using CDF matching approach

Surface soil moisture data from different sources (satellite, ground measurement, land model) typically exhibit very different mean values and variability. These biases possess an obstacle to fully exploit the useful information contained in satellite retrieval through data assimilation technique (Reichle and Koster, 2004). Although, SMAP was calibrated over 8 in situ stations in Core Validation Sites, but these are not within the USCRN stations network at this time of study. Therefore, bilinear interpolation and bias correction approach is required to downscale the resolution and reduce the mismatch between satellite and in-situ observations. Rescaling techniques are used to adjust satellite data to match in situ variability (Brocca et al., 2011). When remote sensing data

are assimilated into a hydrological or meteorological model, they gravitate towards the distributional characteristics of the model prognostics and diagnostics. Combined use of remote sensing and in situ data requires harmonization of the ranges of variability and mean conditions (Liu et al., 2011; Brocca et al., 2010; Entekhabi et al., 2010b; Miralles et al., 2010; Koster et al., 2009). Hence in this study we used the Cumulative Distribution Function (CDF) matching approach, which has been extensively used in bias correction and dynamic range matching of satellite soil moisture and in situ data (Kumar et al., 2012; Brocca et al., 2011; Drusch et al., 2005; Reichle and Koster, 2004). This approach considerably increased the SMOS biases (Lee and Im, 2015). The CDF matching method can be considered as an enhanced non-linear technique for removing systematic differences between two datasets (Brocca et al., 2011).

The procedure for CDF matching is briefly described using following steps: (1) construct the cumulative distribution functions (CDF) for in situ and SMAP soil moisture data, (2) compute the difference ' d_i ' between the CDF of in situ and SMAP soil moisture, (3) the time series of ' d_i ' for all percentiles are approximated using linear interpolation, and (4) add the ranked SMAP soil moisture with newly constructed ' d_i ' from previous step to construct scaled SMAP dataset.

3.2. Soil water deficit index (SWDI)

The Soil Water Deficit Index (SWDI) (Martínez-Fernández et al., 2015) captures drought conditions by quantifying associated soil moisture deficit. We use SWDI to quantify agricultural drought based on the surface soil moisture for the top 5 cm depth, which is useful for drought studies. The SWDI has a direct relation to agriculture drought because it affects the soil moisture suction capacity of different type of crops. SWDI considered to be an effective agricultural drought index, as it is based on soil moisture and basic soil water parameters (Martínez-Fernández et al., 2015, 2016). This drought index is able to adequately identify the main attributes that define an agricultural drought event. The SWDI is calculated using Eq. (1):

$$SWDI = \left(\frac{\theta - \theta_{FC}}{\theta_{AWC}}\right) \times 10 \tag{1}$$

where, θ , θ_{AWC} , θ_{FC} , represents soil moisture (m³/m³) and volumetric water content (m³/m³) at available water capacity (AWC), field capacity (FC) respectively. θ_{AWC} , is calculated by subtracting θ_{FC} with volumetric water content at wilting point (θ_{WP}) as in Eq. (2):

$$\theta_{AWC} = \theta_{FC} - \theta_{WP} \tag{2}$$

When SWDI is positive, the soil moisture content is higher than field capacity, hence, excessive water is available above capillary storage for crop growth. When SWDI is negative, it signifies the drought condition. In this study, the SWDI was computed in weekly time scale similar to Martínez-Fernández et al. (2016) and the drought classification based on SWDI is provided in Table 1. We applied theory of runs (Mishra and Singh, 2010) to calculate drought characteristics, such as percentage of drought events and

Table 1Classification of SWDI for different drought categories (Adapted from Martinez-Fernandez et al., 2015).

SWDI value	Drought category	
≥0	No drought	
0 to −2	Mild	
−2 to −5	Moderate	
−5 to −10	Severe	
≤-10	Extreme	

total drought severity (TDS) using weekly SWDI. The theory of run can be applied to a time series of drought variable (i.e., SWDI and AWD) to identify drought and wet events based on either below or above the selected threshold level (Mishra and Singh, 2010). The percentages of drought events show the severe to extreme drought occurrence (%) during the study period for different stations. The TDS indicates a cumulative deficiency of a drought indicator below the critical level (SWDI ≤ -5 is used in this study).

3.3. Atmospheric water deficit (AWD)

The Atmospheric Water Deficit (AWD) is used to validate the reliability of the SWDI for agricultural drought monitoring. AWD is a suitable index to monitor drought dynamic related to soil water storage (Torres et al., 2013). The AWD is computed based on 7-day water deficit for each day of year (DOY), which is calculated by subtracting 7-day running sum of potential evapotranspiration (ET₀) and precipitation (P) (Purcell et al., 2003). The ET₀ in Purcell et al. (2003) was calculated using the FAO (Food and Agricultural Organization) modified form of the Penman Monteith equation (Allen et al., 1998). Van der Schrier et al. (2011) compared Penman-Monteith and Thornthwaite (Thornthwaite, 1948) approach to compute ET₀ for Palmer Drought Severity Index (PDSI) and concluded that both methods produced similar PDSI values in terms of correlation, regional averages, trends and identifying extremely dry or wet months. Therefore, in this study, ET₀ was computed based on Thornthwaite method as it requires less parameter such as daily mean temperature and station latitude (Thornthwaite, 1948). AWD was reversely computed (P-ET₀) to obtain negative values when precipitation P is less than ET₀ (Martí nez-Fernández et al., 2016). In brief, weekly AWD can be obtained from the following steps (Torres et al., 2013; Purcell et al., 2003): (1) compute daily evapotranspiration (ET₀) using Thornthwaite approach for each station, (2) compute 7-day running sum of rainfall (P) and ET₀ for the study period, (3) then subtract the 7 days running sum time series of ET₀ from P, and (4) finally compute weekly AWD by summing up the daily AWD calculated from previous step. The weekly temporal scale is selected for agriculture drought monitoring as it has been commonly used in irrigation schedule by farmer (Purcell et al., 2003; Mishra et al., 2015). In this study, both AWD and SMAP_SWDI time series are derived at weekly time scale. In Purcell et al. (2003), the drought threshold was set at -50 mm for weekly AWD (using 16 sites over 4 geographical regions in USA). The similar threshold is used in this study.

3.4. Soil water characteristics

This section describes the methodology to derive the volumetric water content at wilting point (θ_{WP}) and field capacity (θ_{FC}). Several approaches are available to estimate these soil water characteristics, such as, laboratory analysis (to experimentally derive water retention curve (van Genuchten, 1980) of unaltered soil monoliths from 0 to 5 cm depth) (i.e. Martínez-Fernández et al., 2016); based on percentiles using long term soil moisture time series (Hunt et al., 2009); or pedotransfer function (PTF) (Bouma and van Lanen, 1987). While the first technique is costly and time consuming, the second approach requires a rather longer time series of soil moisture data to validate the method. Considering these limitations, we utilize the PTF technique (e.g., regression approach) to estimate the θ_{WP} and θ_{FC} based on soil physical characteristics, such as, texture (%Sand, %Silt, %Clay), organic matter and bulk density. PTF is a well-known technique to bridge the gap between soil data and hydraulic characteristics, it has been proven useful in many areas, where there is no availability of soil water parameters (Wosten et al., 2001).

Several PTF regression formulas have been developed, for example, Rawls et al. (1982) formulated the PTF based on 1323 soil samples over 32 states in USA using soil texture, organic matter and bulk density. Batjes (1996) developed the PTF for global soil dataset using soil texture extracted from FAO-UNESCO Soil Map of the World. More recently Saxton and Rawls (2006) developed new soil water characteristics equations based on the USDA soil database consists of soil texture and organic matters. It is an upgraded version from Saxton et al. (1986) with inclusion of large and more reliable data consists of additional variables. In this study, we applied the PTF from Saxton and Rawls (2006) (Eqs. 3 and 4) to derive the soil water characteristics for CONUS based on soil physical characteristic from the top soil layer of FAO Harmonized World Soil Database (HWSD) (FAO, 2009) (at 5 km spatial resolution).

$$\begin{array}{l} \theta_{1500} = \theta_{1500}^* + (0.14 \times \theta_{1500}^* - 0.02) \\ \theta_{1500}^* = -0.024S + 0.487C + 0.006OM + 0.005(S \times OM) \\ -0.013(C \times OM) + 0.068(S \times C) + 0.031 \end{array} \tag{3}$$

$$\theta_{33} = \theta_{33}^* + [1.283(\theta_{33}^*)^2 - 0.374\theta_{33}^* - 0.015]$$

$$\theta_{33}^* = -0.251S + 0.195C + 0.0110M + 0.006(S \times OM)$$

$$-0.027(C \times OM) + 0.452(S \times C) + 0.299$$
(4)

in which:

S: Sand (% weight);

C: Clay (% weight)

OM: Organic Matter (% weight): converted from Organic Carbon by a factor of 0.58 (Pribyl, 2010; Shangguan et al., 2014)

 θ_{1500} : 1500 kPa moisture (or wilting point – volumetric content) θ_{33} : 33 kPa moisture (or field capacity – volumetric content)

 $\theta_{1500}^*, \theta_{33}^*$: 1500 and 33 kPa soil moisture, first solution (volumetric content)

The calculation was carried out at HWSD original spatial resolution then extracted at in situ grid points using bilinear interpolation approach.

3.5. Goodness of fits test

In this study, Pearson correlation coefficient 'R' and Willmott Index of agreement 'd' are used to measure the performance of two time series. It is to be noted that more than one measure for goodness of fits should be reported (Willmott, 1982). The Pearson correlation coefficient 'R' is a popular index to measure the strength of a linear or monotonic relationship between observed data and model output ****(Gan et al., 2014). The Pearson correlations ranges from -1 to 1 and are computed at a 95% confidence level. However it does not account for the dependence of magnitude between the two datasets. Therefore the second index is used to measure the model performance, which is Willmott's index of agreement 'd' (Willmott, 1981), which is calculated as in Eq. (5).

$$d = 1 - \frac{\sum_{i=1}^{n} (M_i - O_i)^2}{\sum_{i=1}^{n} (|M_i - \overline{O}| + |O_i - \overline{O}|)^2}$$
(5)

where M is model and O is observation time series, \overline{O} is the average value of observed soil moisture. The Willmott index values has a range between 0 and 1, with value closer to 1 indicates a better model performance. This index has been widely used in measuring soil moisture performance for many other studies (Qin et al., 2013; Torres et al., 2013).

4. Results and discussion

4.1. Evaluation of SMAP L3 and in situ soil moisture dynamics

Soil moisture plays an important role in agricultural drought management. Therefore as a first step, we evaluated the performance of the SMAP L3 surface soil moisture with respect to USCRN in situ soil moisture at four locations over CONUS. These locations were selected based on different vegetation from Modis Global Land cover (Broxton et al., 2014) and different climate regimes from Koppen climate type (Koppen, 1900; Rubel and Kottek, 2010) and are similar to the study by Pan et al. (2016). The detail vegetation/climate region for each location is tabulated in Table 2. The daily time series of soil moisture from SMAP and in situ observations are plotted along with precipitation (shown in Fig. 1), and the their performance was evaluated using Pearson correlation coefficient (R) and Willmott Index of agreement (d). It was observed that the SMAP and in situ soil moisture follow closely with precipitation events. The consistency between SMAP and in situ soil moisture data differs based on the climate (vegetation) regimes, for example, a reasonable performance was observed for Austin, Texas (Fig. 1c) based on high correlation 'R' (0.89), however. it has lower Willmott index 'd' (0.67) in comparison to stations Bowling Green, KY (Fig. 1b) and Coshocton, OH (Fig. 1d). The possible reason for comparatively low 'd' at Austin may be due to SMAP soil moisture underestimates the peak of in situ observations for the events in May 2015 and Nov 2015 to Feb 2016. Even though SMAP data captures fairly well the linear relationship with in situ soil moisture and precipitation events, the comparatively low 'd' is mainly attributed to mismatch in peak values. Higher inconsistency between SMAP and in situ soil moisture data was observed for station Los Alamos, NM (Fig. 1a) based on low correlation (R = 0.14) and Willmott index (d = 0.42). However, the SMAP soil moisture data is able to capture the in situ peak values for few months, except during January to April months.

Based on the previous discussion it was observed that there is an inconsistency pattern exists between SMAP L3 and in situ soil moisture time series and it varies with respect to climate (vegetation) regimes. This inconsistency between two time series will lead to inaccurate in situ drought information based on original SMAP L3 soil moisture data. Therefore, bias correction technique using CDF rescaling approach was applied to rescale the SMAP L3 time series to match with in situ soil moisture observations.

As an example, the application of CDF rescaling approach for SMAP L3 product using in situ dataset at Austin station (TX) and Los Alamos (NM) is shown in Fig. 2. The rescaled SMAP L3 data for Austin (red dashed line in Fig. 1a1) matches well with in situ soil moisture observations (black line), when compared to original SMAP L3 data (blue line). The soil moisture time series at daily time scale based on original, rescaled SMAP and in situ observation for the station located at Austin (TX) is shown in Fig. 2b1. Black continuous line indicates in situ soil moisture at 5 cm; green circle represents the original SMAP L3 soil moisture at top 5 cm; while red points show the Bias corrected SMAP L3 soil moisture time series. It was observed that the rescaling approach harmonizes the mean and amplitude of variations and SMAP L3 satisfactorily captures in situ soil moisture pattern. The scatter plot between original and bias corrected SMAP is provided in Fig. 2c1 and the RMSE are significantly improved by reducing from 0.15 to 0.06 (m³/m³). In contrast to Austin, the SMAP poorly performed over Los Alamos station. The rescaled SMAP's CDF matches well with in situ data (Fig. 2a2), whereas there is a large mismatch between original SMAP and in situ (Fig. 2b2) observation. This suggests that the rescaled SMAP can improve the RMSE values as seen in Fig. 2c2.

 Table 2

 Goodness of fits ('d' and 'R') comparison between selected drought indices (The values in brackets are computed based on 1-week lag time of SWDI with AWD).

Station/State	Vegetation/Koppen Climate type	Willmott Index of agreement 'd'	Pearson correlation coefficient 'R'	
		In-situ SWDI & SMAP_SWDI	In-situ SWDI & SMAP_SWDI	SMAP_SWDI & AWD
Los Alamos NM	Grass land/Cfc	0.35	-0.02	0.45 (0.43)
Bowling Green KY	Deciduous Broadleaf Forest/Cfa	0.87	0.77	0.17 (0.48)
Austin TX	Savannas/Cfa	0.96	0.92	0.56 (0.84)
Coshocton OH	Cropland & Natural Vegetation Mosaic/Cfa, Dfa	0.81	0.65	0.30 (0.61)

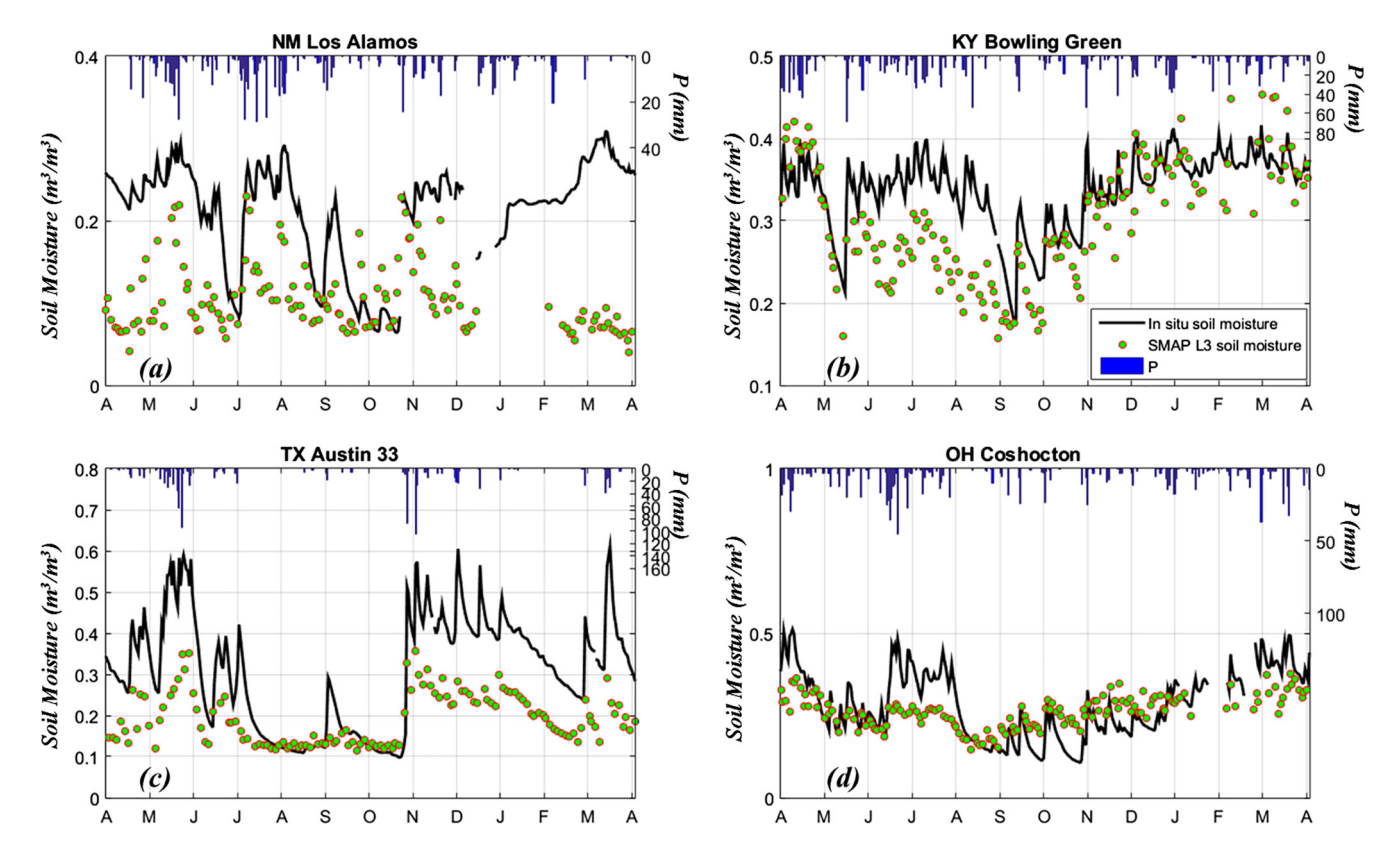


Fig. 1. Daily in-situ and satellite (SMAP L3) soil moisture estimates along with precipitation observation for stations: (a) Los Alamos-NM (R = 0.14; d = 0.42) (b) Bowling Green-KY (R = 0.73; d = 0.74) (c) Austin-TX (R = 0.89; d = 0.67) (d) Coshocton-OH (R = 0.63; d = 0.69). (For interpretation of the references to color in this figure legend, the reader is referred to the web version of this article.)

Taylor diagram in Fig. 3 compares the performance of rescaled SMAP and in situ soil moisture data at daily time scale based on 104 USCRN stations located in CONUS. The average correlation coefficient value using all the stations found to be 0.67. This is relatively higher than the correlation between soil moisture from Advanced Microwave Scanning Radiometer–EOS (AMSR-E) products over CONUS with CRN and SCAN in situ network (around 0.48–0.56) (Pan et al., 2014, 2016).

4.2. Estimation of the SWDI

The weekly SWDI time series is derived based on in-situ, original and rescaled SMAP L3 soil moisture datasets for 104 USCRN stations spreading over CONUS. First, the SWDI was computed at daily time scale, and then it was aggregated to weekly temporal scale. This approach is similar to Martínez-Fernández et al. (2016), where they applied the SMOS dataset to compute SWDI. The SWDI time series obtained from in situ and original (rescaled) SMAP soil moisture data was compared with AWD at four selected stations (Fig. 4). A broad range of scenario was observed based on agreement (disagreement) between SWDI derived from three different sources of information (e.g., in situ, original and rescaled).

The temporal patterns and typology of differences are informative for applying SMAP data for drought analysis. Among these four locations, best match was observed for Austin, TX (Fig. 4c) and relatively poor performance was observed at Los Alamos, NM (Fig. 4a). The deficit of rainfall was clearly captured by SWDI based on its higher negative values during 2015 and 2016 drought events. For example, the lack of precipitation during June to November 2015 at Austin, TX (Fig. 4c) led to extreme drought conditions as the SWDI values reduced to nearly -20 from mid-July to November 2015 (weekly AWD also reduced to less than -150 mm). The SWDI and AWD values increase in mid-November when higher amount of rainfall observed in first week of November 2015, then gradually reduce to approximately zero for the subsequent 3 months. The severe drought period shown in Fig. 4c for Austin (TX) agrees well with a previous study (Velpuri et al., 2016). In the previous study (Velpuri et al., 2016), the authors compared average SMAP soil moisture for the two month Sep-Oct 2015 with US Drought Monitor weekly data and observed that the reduction of soil moisture coincides with extreme drought during the first three weeks of October 2015. This drought condition was resolved by a heavy rainfall by the last week of October that led to the soil moisture value to normal condition.

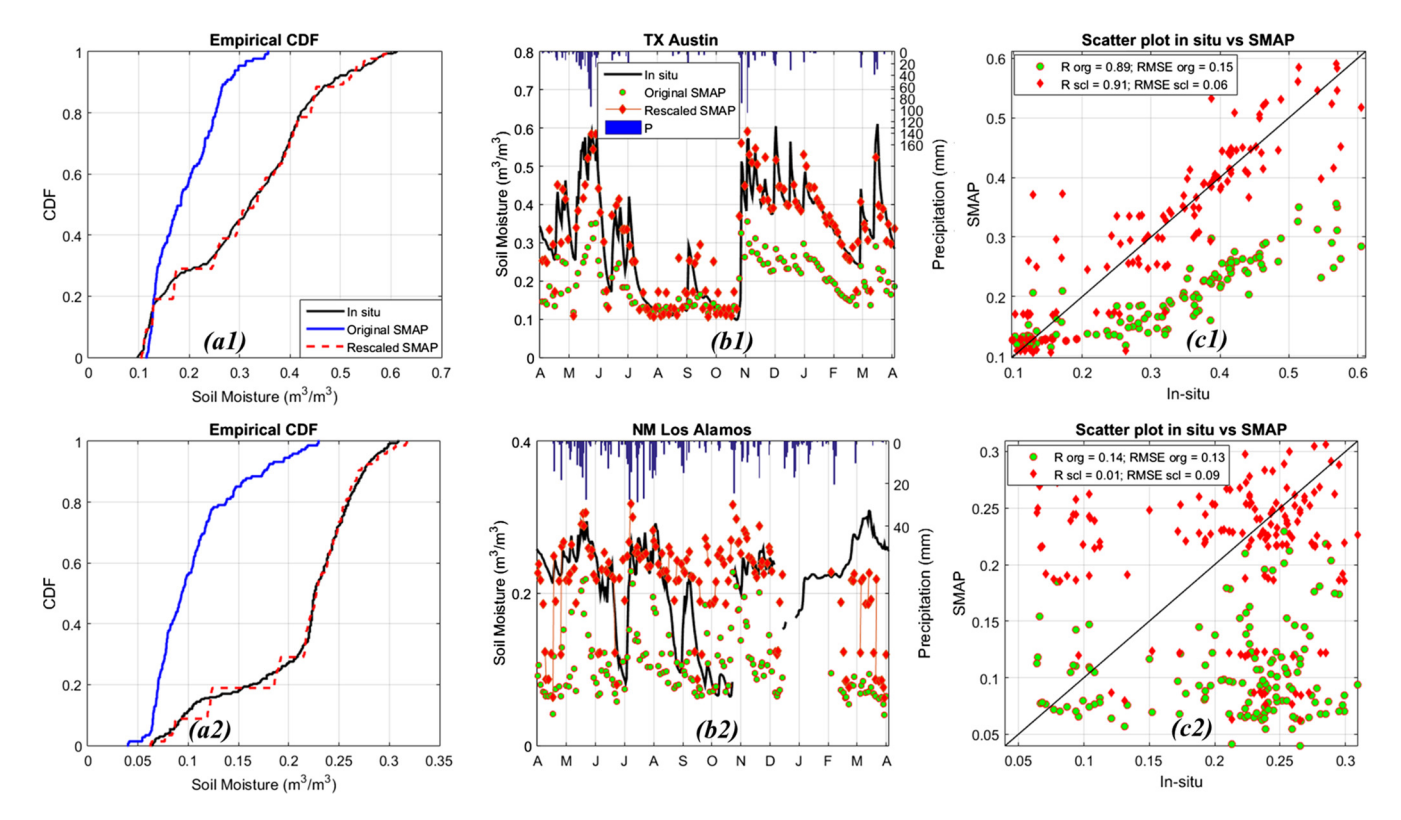


Fig. 2. (a) Cumulative Distribution Function (CDF) based on in-situ, original and rescaled SMAP L3, (b) time series plot of original and rescaled SMAP L3 soil moisture data at top 5 cm depth, and (c) scatter plot between original (org) and rescaled (scl) SMAP L3 data with respect to in-situ observations for station (1) Austin, TX (2) Los Alamos, NM.

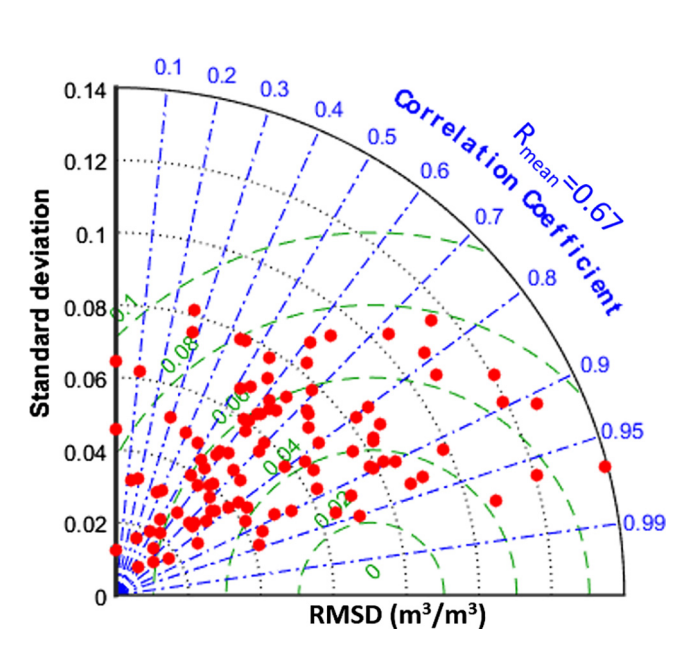


Fig. 3. Taylor diagram comparing the performance of rescaled SMAP and in situ soil moisture over 104 USCRN stations for study period 2015/04–2016/03. Correlation coefficient is represented by blue dashed dotted line while RMSD is displayed by green dashed line. (For interpretation of the references to color in this figure legend, the reader is referred to the web version of this article.)

Similar information was captured (Fig. 4c) by the weekly SWDI for in situ and rescaled SMAP data during the first week of November 2015. However, the raw SMAP_SWDI (represented in dashed grey color), due to its bias, is only able to indicate an increasing in soil moisture, but to the level of SWDI equals to '-8' (severe drought).

The comparison based on Willmott index (d) and correlation coefficient (R) between in situ SWDI, SMAP_SWDI and AWD at four

locations are provided in Table 2. It was observed that the Willmott 'd' and correlation 'R' values indicate good agreement (d > 0.8: R > 0.65) between rescaled SMAP_SWDI and in situ SWDI at three locations except Los Alamos (NM). This may be perhaps due to the difference between the in situ and the SMAP soil moisture dynamics as well as the possible missing data retrieved from satellite swath paths. The lower goodness of fits ('d' and 'R') between in situ and SMAP_SWDI time series are likely to influence drought characteristics, such as, drought severity and percentage of drought events, which will be discussed in the latter Section 4.4. Also as seen in Table 2, the 'R' values between rescaled SWDI and AWD are significantly better with 1-week lag time compared to without lag (displayed in brackets in Table 2), at three sites except Los Alamos (NM). It is expected that the 1-week lag time between SWDI and AWD likely to have higher correlation in comparison to without lag time and similar finding was observed in Martínez-Fernández et al. (2015) but for SMOS_SWDI with in situ in Spain. Even though, the relationship between in situ and SMAP based SWDI might be poor, the performance can improve with respect to other drought indices. For example, the station located in Los Alamos witnesses a poor correlation (-0.02) between in situ and SMAP based SWDI, however comparatively better correlation exists between SMAP_SWDI with AWD (R = 0.43). The higher correlation between SMAP_SWDI and AWD (R = 0.84) was observed for station located at Austin, TX.

4.3. Comparison between SMAP SWDI and AWD over CONUS

We compared in situ (SMAP) based SWDI and AWD for 104 in situ stations located in diverse climatic (vegetation) regions spread across CONUS. As a first step we compared SWDI derived based on in situ observations and SMAP L3 information based on Willmott 'd' and Pearson 'R' (Fig. 5). The comparison between these indices are classified into three groups (similar to Albergel et al.

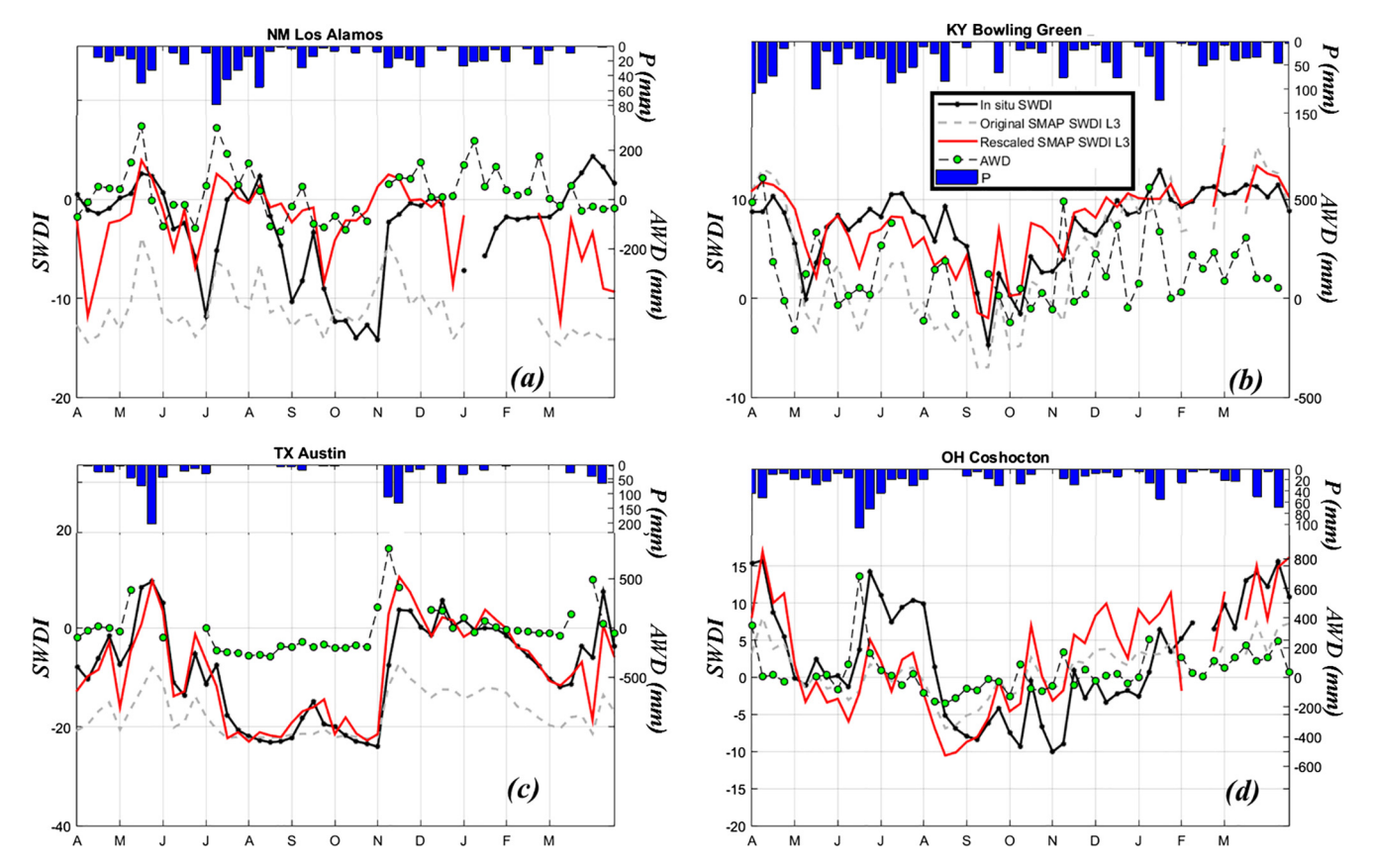


Fig. 4. Time series plot of weekly in-situ AWD and weekly SWDI derived based on in-situ and bias corrected SMAP L3 soil moisture data for four stations: (a) Los Alamos-NM (b) Bowling Green-KY (c) Austin-TX (d) Coshocton-OH. (For interpretation of the references to color in this figure legend, the reader is referred to the web version of this article.)

(2012) based on correlation coefficients): Best (values higher or equal to 0.7): Fair (values range between 0.5 and 0.7), and Poor (values less than or equal to 0.5). This proposed classification could be different and in general they are experience-based levels of performance that are applicable in this context (Entekhabi et al., 2010b). As seen in Fig. 5a, it was observed that the correlations are statistically significant (p < 0.05) for more than 85% selected stations since the precipitation storms and dry-downs as well as seasonality are probably both well-captured by the in situ and SMAP L3 radiometer data. This may be possible since the wet and dry spells as well as seasonality are reasonably captured well by SMAP L3 with respect to in situ data. It was observed that nearly 85% and 60% of the selected stations performed best (index > 0.7) based on Wilmott Index of agreement and Pearson correlation coefficient respectively (Fig. 5a, b). This observation is similar to Pan et al. (2016) where the fair to best correlation coefficients (R > 0.5) are observed for most part in CONUS (Fig. 5b), except for few locations on the east coast and some isolated pockets in the Rocky Mountains. The poor performance was observed for 15% and 40% of the stations based on the Wilmott Index of agreement and Pearson correlation coefficient respectively and they are concentrated around the higher topography areas such as in the central parts around Rocky Mountain and Great Plains region. The average value of 'd' and 'R' based on 104 stations are 0.82 and 0.7 respectively which indicates the improvement made by bias corrected data.

The performance of 1 week delayed SMAP_SWDI and AWD were compared based on Pearson correlation (R) for 104 in situ stations (Fig. 6). The poor correlation values (R \leq 0.5) between 1-week lag SMAP_SWDI and AWD are found in the regions mostly located around Great Plains and along US east coast (similar locations as in

Fig. 5b). Approximately 75% of the stations performed reasonably well (R > 0.5) based on the correlation between SMAP_SWDI and AWD (Fig. 6). Similar range of correlations is found based on quality controlled 1-week delay SMOS_SWDI with AWD in Martínez-Fernández et al. (2015).

4.4. Assessment of drought characteristics over CONUS

4.4.1. Percentage of drought event

Percentage of drought event was calculated based on the ratio between numbers of weeks under severe drought divided by the total number of weeks for the study period, subsequently multiplied by 100 to obtain the percentage (%). This ratio represents the percentage of time that the location is under drought condition. In this study, we only evaluated severe to extreme drought events which are identified by predefined threshold, for example, -5 is used as threshold to quantify severe and extreme droughts for SWDI and -50 mm as a threshold for AWD. The spatial distribution of percentage of drought event based on SMAP_SWDI and AWD are shown in Fig. 7a and b respectively. For comparison between these three selected indices, we classified the percentage of drought events (P) into four groups: (1) P < 25% (i.e., it represents less than 12 weeks of drought events), (2) 25% < P < 50% (3) 50% < P < 75%, and (4) P > 75% (i.e., it represents more than 37 weeks of drought events). The percentage of stations corresponding to each aforementioned group is calculated based on the total number of 104 stations used in this study (Fig. 7). These two drought indices indicates higher percentage of drought events in the western US during the study period. The difference between these two drought indices was observed based on the percentage of drought, for example, SMAP_SWDI has fair amount of ratio

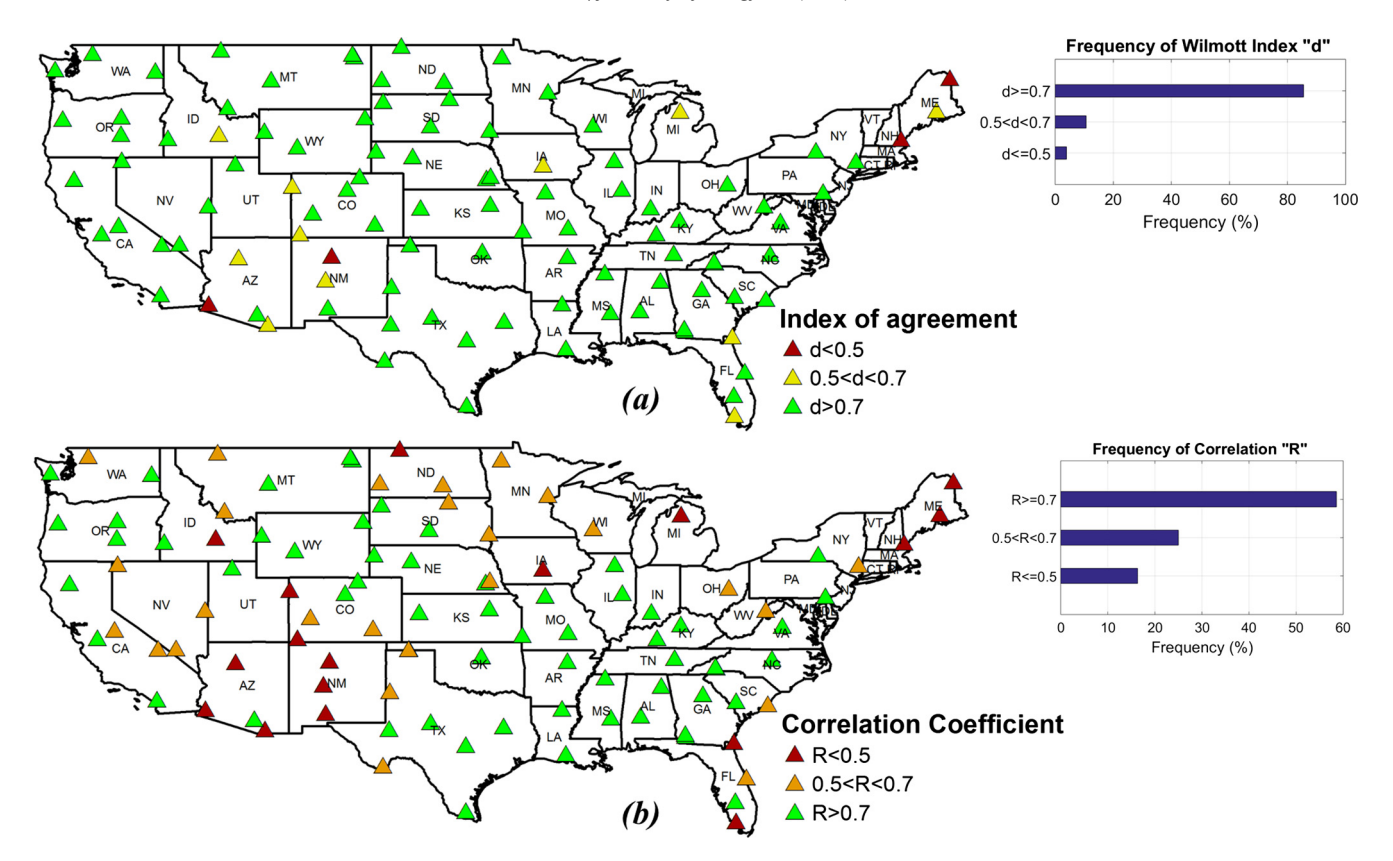


Fig. 5. (a) Wilmott Index of agreement (d), and (b) Pearson correlation coefficient (R) between weekly SMAP_SWDI and in-situ based SWDI at 104 stations. [Note: The average "d" over CONUS is 0.82 and average "R" over CONUS is 0.7 based on the 104 selected stations]

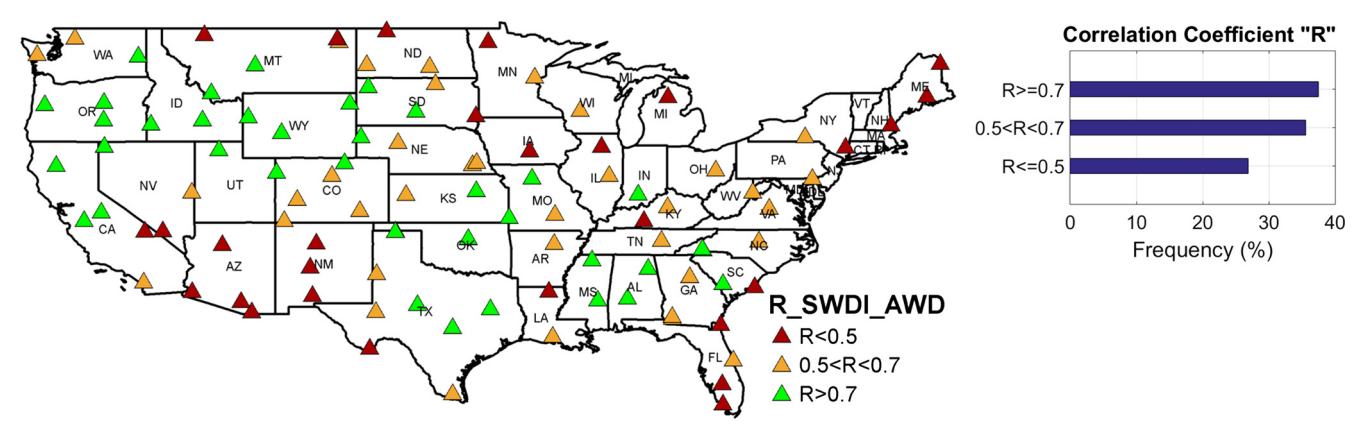


Fig. 6. Pearson correlation coefficient (R) between weekly SMAP_SWDI (lag 1 week) and AWD. The average "R" over CONUS is 0.58.

(\sim 20%) for the first three categories and about 40% of stations having less than 12 weeks (<25%) under drought (Fig. 7a). On the other hand, AWD has most of the stations (> 60%) witness moderate drought events and less number of stations witness droughts for longer period (Fig. 7b). However, both indices do have common stations for percentage of drought event less than 25%, distributed along east coast as well as percentage higher than 50% along the southern states spanning from California to Texas.

4.4.2. Drought severity

Total Drought Severity (TDS) was calculated based on SMAP_SWDI and AWD for 104 stations during the study period are shown in Fig. 8. The TDS was computed at weekly time scale based on the accumulation of deficit below the truncation levels.

Because SWDI and AWD have different drought deficit magnitude, therefore in order to compare the TDS among spatially distributed stations, we classified the stations based on absolute TDS into four groups by applying quartile technique (75th, 50th and 25th percentile) (Fig. 8): Extreme drought severity (>75th percentile), Severe drought severity (50th to 75th percentile), Moderate drought severity (25th to 50th percentile), mild drought severity (<25th percentile). It is worth to mention that the quartiles represented in Fig. 8 are based on spatial distribution of stations. The distributions of TDS for SWDI and AWD look quite similar (Fig. 8). The spatial distribution of stations for selected drought indices indicates severe to extreme drought (>50th of TDS) along Rocky Mountain to Great Plains, west coast to southern US and several stations in Florida. This is consistent with previous findings that droughts

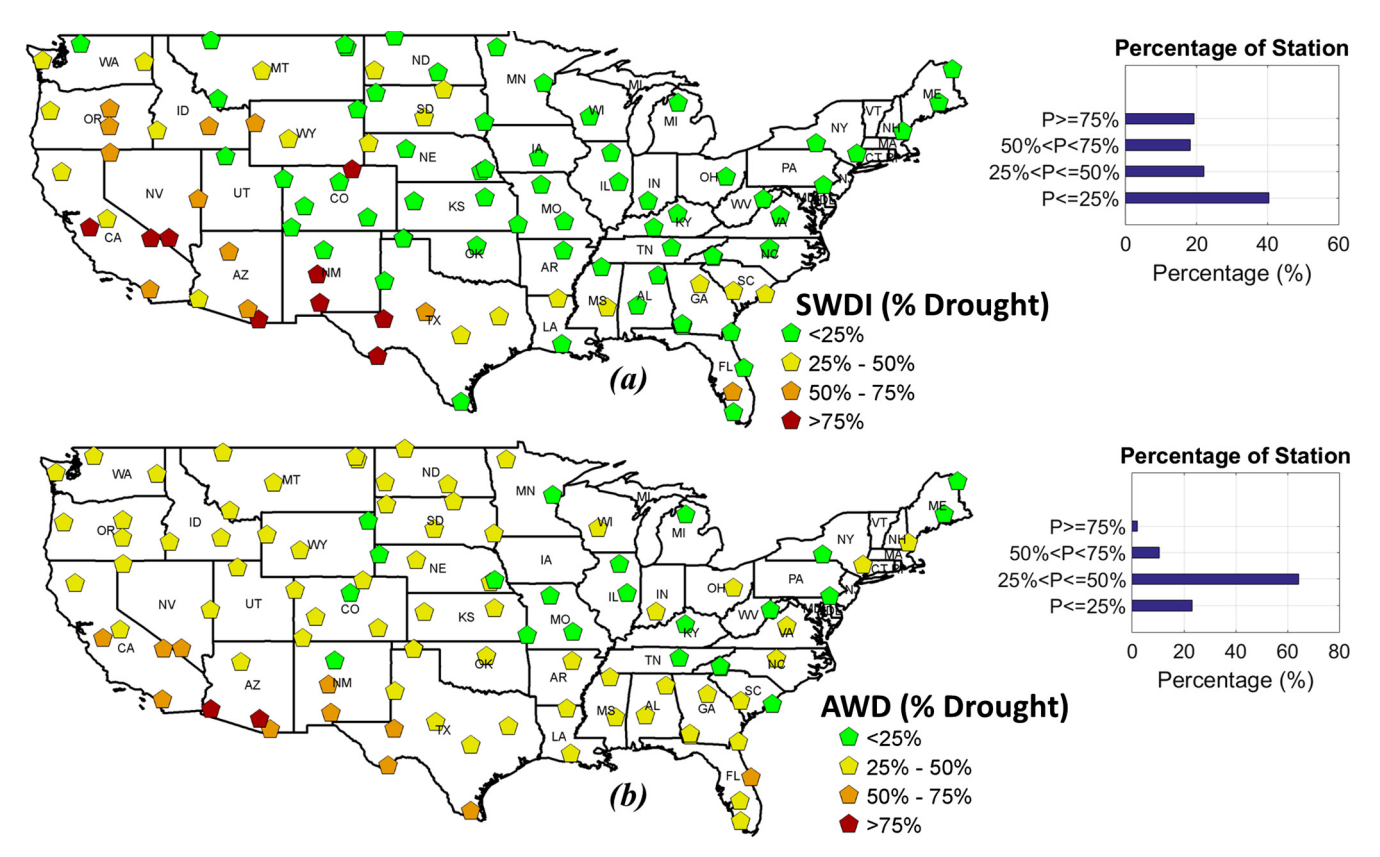


Fig. 7. Percentage of drought event (%) based on (a) SMAP_SWDI, and (b) AWD.

tend to be more persistent in the interior sections of the CONUS, particularly the central to northern Great Plains and Rocky Mountains, in comparison with the remainder of the country (Andreadis et al., 2005; Soule, 1992; Karl and Koscielny, 1982; Walsh et al., 1982). It is clearly seen that the eastern and northeastern CONUS has less Total Drought Severity than the western part of CONUS over the study period.

4.5. Agricultural drought mapping for CONUS

The spatial distribution of mean value of SMAP soil moisture over CONUS for the month September 2015 is provided in Fig. 9a. It can be observed that the western part of CONUS have lower soil moisture values in comparison to the central and eastern regions. Most importantly, this figure also reflects the soil moisture gradient across the CONUS. The distinct wet and dry soil moisture region is divided along the states of Minnesota, Iowa, Kansas, Oklahoma and Texas (from north to south) as seen in Fig. 9a. However, it is difficult to quantify the agriculture drought for the particular month/week by analyzing the spatial distribution of soil moisture. Therefore, the SWDI is used to construct agricultural drought maps to quantify spatial drought pattern for the CONUS. The calculation of SWDI depends on the soil parameters such as available water capacity (θ_{AWC}) and Field Capacity (θ_{FC}). Lack of adequate AWC information is one of the major limitations for agricultural drought monitoring based on short satellite records. It is important to generate accurate values of θ_{FC} and θ_{WP} for CONUS that can match spatial resolution of SMAP. We obtain soil parameters (θ_{AWC} and θ_{FC}) from pedo-transfer function using HWSD soil characteristics (% Clay, %Sand, Organic Matter) and they are re-gridded to match SMAP data posting.

The spatial distribution of SMAP_SWDI (Fig. 9b) is similar to the SMAP soil moisture distribution (Fig. 9a). However, instead of dis-

playing the soil moisture value in volumetric content unit, the SMAP_SWDI depicts the severity of drought (from mild drought to extreme drought). Severe and extreme droughts in September 2015 are observed over western and central part of CONUS. In addition, the SMAP SWDI is also compared with existing drought indices, such as, monthly AWD (Fig. 9c), self-calibrating Palmer Drought Severity Index (sc-PDSI; downloaded from https:// crudata.uea.ac.uk/cru/data/drought/) (Fig. 9d), Palmer Z index (Fig. S1a - in Supplementary) and Standardized Precipitation Evapotranspiration Index (Fig. S1b - in Supplementary) (SPEI, Vicente-Serrano et al., 2010). Because each drought index has its own range (for example SWDI ranges from -10 to 0; sc-PDSI ranges from -4 to 4) and drought threshold, thus for simplicity, in this study, we classify these indices in terms of nature of drought (from mild drought to extreme drought) as displayed in Fig. 9 and S1. Brief discussions on selection of these drought indices are presented.

The gridded AWD was computed based on daily precipitation and temperature from Climate Prediction Center 0.5° global product. The data can be downloaded from ftp site: "ftp://ftp.cdc.noaa.gov/Datasets/". Gridded weekly AWD was computed following the procedure discussed in Section 3.3. The monthly AWD was averaged from weekly AWD and demonstrated in Fig. 9c. At a glance, the spatial drought pattern for AWD product is similar to SMAP SWDI in capturing the severe and extreme drought in western and central part of CONUS as well as some of the wet states over northeastern CONUS and Florida.

Two Palmer's drought indices are selected for comparison because it enables measurement of both wetness and dryness based on the concept of supply and demand using the water balance equation from prior precipitation, moisture supply, runoff and evaporation demand at the surface level (e.g., Karl, 1986; Alley, 1984). For example, the Palmer Z-Index is an agricultural

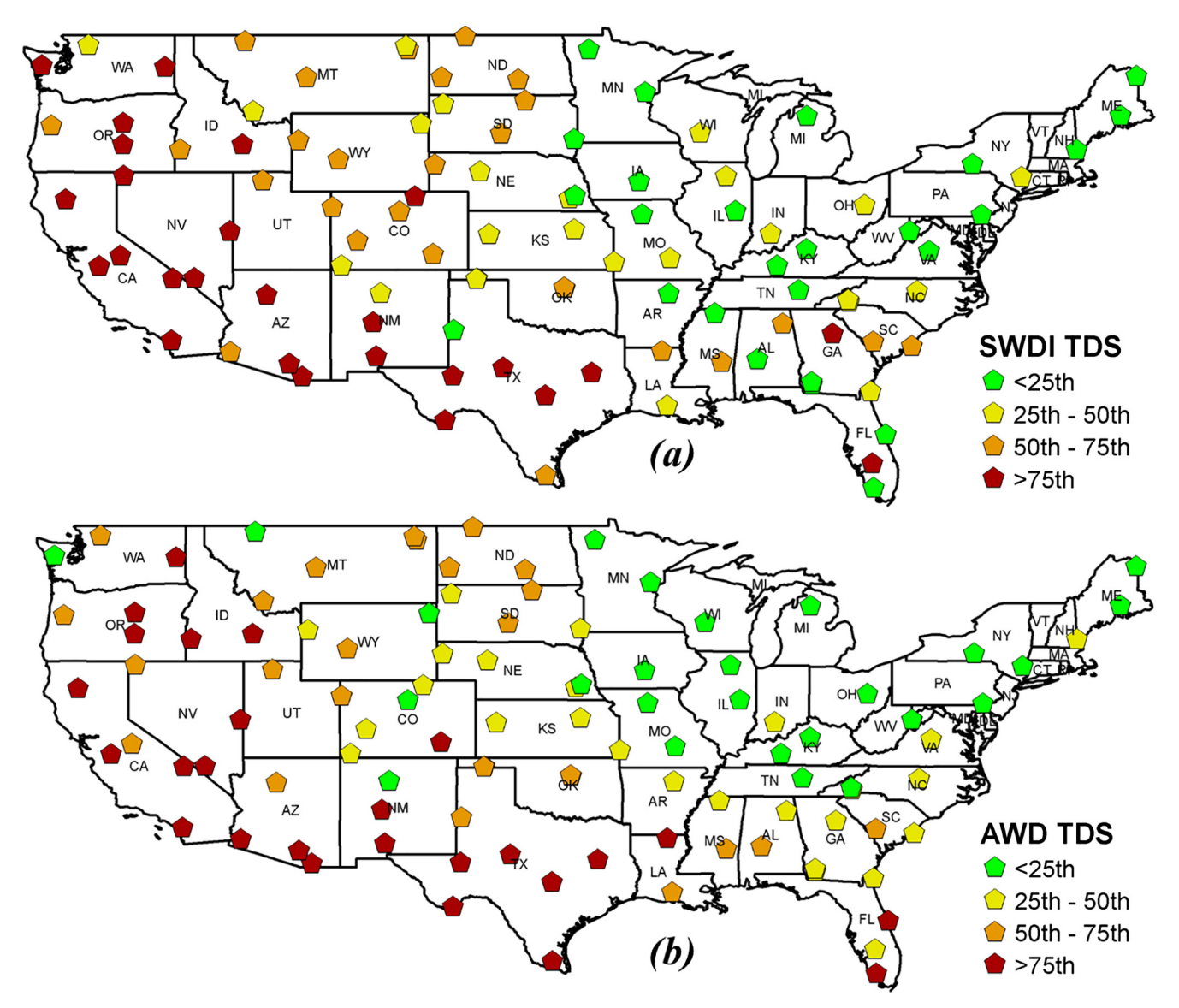


Fig. 8. Total Drought Severity (TDS) based on (a) SMAP_SWDI, and (b) AWD.

drought index and it reflects the monthly, short-term soil moisture anomaly. The sc-PDSI was introduced by Wells et al. (2004) with its main purpose to compare drought characteristics from different climate regimes. The sc-PDSI can better capture the activity of natural vegetation as well as variability in crop production when compared with the SPEI. The SPEI is based on a water balance model that is integrated monthly (or weekly) (Vicente-Serrano et al., 2010). SPEI integrates the sensitivity of sc-PDSI to changes in evaporation demand. In this study, we selected short time scale (i.e., SPEI 1) for comparison as it can better reflects soil water content (Mishra and Singh, 2010) as an proxy for as monitoring agricultural droughts.

In this study we show the example maps of September 2015 which is about the peak of the extended drought covering CONUS recently. Based on spatial comparison, there is agreement (disagreement) among drought indices. Using sc-PDSI, extreme droughts are clustered in the western part and northeastern part of US (Fig. 9d), however Z-Index (Fig. S1a) indicates extreme droughts in Southern part of US (Fig. S1a). This indicates a clear difference in spatial pattern of droughts based on these two drought indices, even though both are useful for agricultural drought study. The information content in these two indices is

useful as sc-PDSI is able to recognize long-term agricultural drought, whereas, Z-Index corresponds to short-term (monthly) agricultural drought conditions with no memory to previous monthly deficits or surpluses. The SMAP based SWDI (SMAP_SWDI) captures spatial drought areas that are present in sc-PDSI and Palmer Z index in the western and southern part of US (Fig. 9d and S1a). The SMAP_SWDI adds spatial details that are not present in the current drought products. SPEI 1 is also able to capture most of spatial drought information available in sc-PDSI and Z-Index. There is a reasonable agreement between SMAP_SWDI and SPEI 1 (Fig. 9b and S1b) based on their spatial drought patterns. In comparison to SPEI 1, the SMAP-SWDI better captures the nature (e.g., extreme vs. moderate) of drought indicated by sc-PDSI and Z-Index.

As agricultural drought indices, the SMAP_SWDI captures short term moisture information from AWD and Z-Index (where past month has no influence) as well as long term information from sc-PDSI (where antecedent conditions accounts two-thirds of its value). More importantly it can add valuable mapping capability with finer scale detail than available in current drought maps. SMAP-SWDI is able to capture drought information at higher spatial resolution, which can be used to better inform local stakehold-

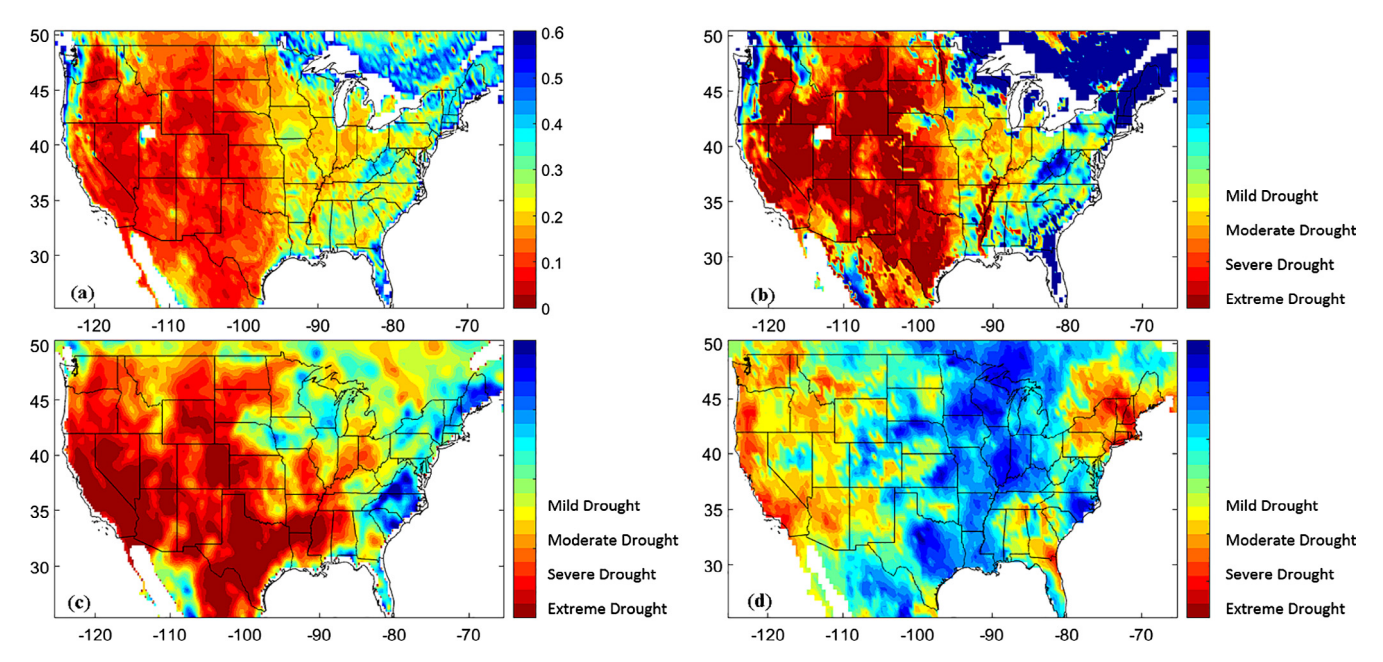


Fig. 9. Spatial map of (a) Average SMAP soil moisture (m³/m³), (b) SMAP_SWDI, (c) AWD, and (d) sc-PDSI over CONUS for the month of September 2015.

ers responsible for developing water management strategies and policies.

5. Conclusions

In this study, we investigated the potential application of Soil Moisture Active Passive (SMAP) information for agricultural drought study. Agricultural drought is quantified using the Soil Water Deficit Index (SWDI) based on SMAP and soil properties (field capacity and available water content) information and compared with Atmospheric Water Deficit (AWD) Index. The following conclusions are drawn from this study:

- (1) The performance of original SMAP L3 passive radiometer volumetric soil moisture data to capture in situ soil moisture dynamics varies with respect to climate (vegetation) regimes. This inconsistency between two time series can possibly lead to inaccurate drought estimation. However, the performance of SMAP L3 can be satisfactorily used to monitor agricultural drought at field (in situ) scale by using suitable rescaling approach.
- (2) Due to the availability of short data record (SMAP launched in Jan 2015), the applications of SMAP for agricultural drought studies can be limited based on the standardized drought indices (e.g., Standardized Soil Moisture Index, etc.), which are derived based on the anomalies of long term data sets. To overcome this limitation SWDI can be used as an agriculture drought index that is derived based on the soil water characteristics (i.e., Field capacity and Available water content). The formulation of SWDI does not depend on longer data and it will overcome the limited (short) length of SMAP data for agricultural drought studies.
- (3) In this study we followed three steps to derive SMAP based SWDI (SMAP_SWDI): (a) first rescale the SMAP L3 passive radiometer soil moisture data to harmonize its average and amplitude of variations with co-located in situ data, (b) then pedo-transfer function (PTF) is used to compute soil water characteristics based on soil texture at the selected location, and (c) the information obtained from steps (a & b) are used as inputs to develop SMAP_SWDI time series. SMAP_SWDI

- can be a good agricultural drought indicator as it is able to capture information content in AWD with 1-week delay temporal scale. SMAP_SWDI can be able to capture drought information, which can be used to better inform local stakeholders responsible for developing water management strategies and policies. The results of this study open the path for using SMAP soil moisture products in drought monitoring. The key challenge is quantifying the soil texture, soil water characteristics as well as long-term marginal probability distribution information required for transforming soil water content into meaningful drought indices. However, more studies are necessary when long-term SMAP data are available.
- (4) The performance of SMAP_SWDI was evaluated with AWD as a reference indicator. The AWD can capture soil water storage dynamics and it is derived based on the concept of water balance model. In this study, we selected short time scale (i.e., weekly) for comparison as it can better reflect soil water content as a proxy for monitoring agricultural droughts. The spatial distribution of drought severity for CONUS based on SMAP_SWDI and AWD looks quite similar, for example, both drought indices are able to capture severe to extreme drought events along Rocky Mountain to Great Plains, west coast to southern part of US and few locations in Florida.
- (5) SMAP_SWDI can be a good agricultural drought indicator as it is able to capture information content compared to AWD, Palmer Z-Index, sc-PDSI and SPEI 1. SMAP_SWDI is able to capture short term moisture information similar to AWD, Z-Index (where past month has no influence) as well as long term information from sc-PDSI (where antecedent conditions accounts two-thirds of its value). This integrated short and long-term information can make SMAP_SWDI a robust agricultural drought indicator. SMAP_SWDI is able to capture drought information at higher spatial resolution, which can be used to better inform local stakeholders responsible for developing water management strategies and policies. However, more studies are necessary when long-term SMAP data are available.

The results of this study open the path for using SMAP soil moisture products in drought monitoring. The SMAP instruments

and satellite operations are optimized to produce global maps of soil moisture. This source of information on soil moisture is a valuable complement to the sparse in situ soil moisture networks and land surface modeling alone. The mapping capability of soil moisture remote sensing opens a new window on the onset and evolution of regional droughts. The key challenge is quantifying the soil characteristics (wilting point and field capacity) as well as long-term marginal probability distribution information required for transforming soil water content into meaningful drought indices.

Acknowledgement

Authors wish to thank anonymous reviewers and editor for their suggestions that helped us to improve our manuscript. This study was supported by the United States Department of Agriculture (USDA) award 2015-68007-23210 and National Science Foundation (NSF) grant # 1653841. Authors would like to thanks NASA for giving free access to SMAP model datasets (http://smap.jpl.nasa.gov/) and USCRN for in situ datasets (https://www.ncdc.noaa.gov/crn/). This study analyzes only existing data, and no new data is created. All data used this paper are properly cited and referred to in the reference list.

Conflict of Interest (COI): Authors do not have COI for their manuscript.

Appendix A. Supplementary data

Supplementary data associated with this article can be found, in the online version, at http://dx.doi.org/10.1016/j.jhydrol.2017.07.033.

References

- Ahmadalipour, A., Moradkhani, H., Svoboda, M., 2016. Centennial drought outlook over the CONUS using NASA-NEX downscaled climate ensemble. J. Climatol Int. http://dx.doi.org/10.1002/joc.4859.
- Albergel, C., de Rosnay, P., Gruhier, C., Muñoz-Sabater, J., Hasenauer, S., Isaksen, L., Kerr, Y., Wagner, W., 2012. Evaluation of remotely sensed and modelled soil moisture products using global ground-based in situ observations. Remote Sens. Environ. 118, 215–226. http://dx.doi.org/10.1016/j.rse.2011.11.017.
- Allen, R.G., Pereira, L.S., Raes, D., Smith, M., 1998. Crop evapotranspiration: Guidelines for computing crop water requirements. FAO Irrig. and Drainage Paper 56. FAO, Rome.
- Alley, W.M., 1984. The Palmer drought severity index: limitations and assumptions. J. Clim. Appl. Meteorol. 23, 1100–1109.
- Anderson, M.C., Hain, C., Otkin, J., Zhan, X., Mo, K., Svoboda, M., Wardlow, B., Pimstein, A., 2013. An intercomparison of drought indicators based on thermal remote sensing and NLDAS-2 simulations with U.S Drought Monitor classifications. J. Hydrometeor. 14, 1035–1056. http://dx.doi.org/10.1175/JHM-D-12-0140.1.
- Andreadis, K.M., Clark, E.A., Wood, A.W., Hamlet, A.F., Lettenmaier, D.P., 2005. Twentieth-century drought in the conterminous United States. J. Hydromet. 6, 958–1001. http://dx.doi.org/10.1175/JHM450.1.
- Bartalis, Z., Wagner, W., Naeimi, V., Hasenauer, S., Scipal, Bonekamp, H., Figa, J., Anderson, C., 2007. Initial soil moisture retrievals from METOP-A advanced Scatterometer (ASCAT). Geophys. Res. Let. 34, L20401. http://dx.doi.org/ 10.1029/2007GL031088.
- Batjes, N.H., 1996. Development of a world data set of soil water retention properties using pedotransfer rules. Geoderma 71, 31–52.
- Bell, J.E., Palecki, M.A., Baker, C.B., Collins, W.G., Lawrimore, J.H., Leeper, R.D., Hall, M.E., Kochendorfer, J., Meyers, T.O., Wilson, T., Diamond, H.J., 2013. U.S. Climate Reference Network soil moisture and temperature observations. J. Hydrometeorol. 14, 977–988. http://dx.doi.org/10.1175/JHM-D-12-0146.1.
- Bouma, J., van Lanen, H.A.J., 1987. Transfer functions and threshold values: from soil characteristics to land qualities. In: Beek, K., Burrough, P.A., McCormack, D., (Eds.), Quantified land evaluation procedures. ITC Pub. No. Vol. 6. The Netherlands: Enschede, pp. 106–110.
- Brocca, L., Hasenauer, S., Lacava, T., Melone, F., Moramacrco, T., Wagner, W., Dorigo, W., Matgen, P., Martinez-Fernandez, J., Llorens, P., Latron, J., Martin, C., Bittelli, M., 2011. Soil moisture estimation through ASCAT and AMSR-E sensors: An intercomparison and validation study across. Eur. Remote Sens. Environ. 115, 3390–3408. http://dx.doi.org/10.1016/j.rse.2011.08.003.
- Brocca, L., Melone, F., Moramarco, T., Morbidelli, R., 2010. Spatial-temporal variability of soil moisture and its estimation across scales. Water Resour. Res. 46, W02516. http://dx.doi.org/10.1029/2009WR008016.

- Brown, M.E., Escobar, V., Moran, S., Entekhabi, D., O'Neil, P.E., Njoku, E.G., Doorn, B., Entin, J.K., 2013. NASA's soil moisture Active Passive (SMAP) Mission and opportunities for application users. Bull. Ams. Met. Soc., 1125–1128
- Broxton, P.D., Zeng, X., Sulla-Menashe, D., Troch, P.A., 2014. A global land cover climatology using MODIS data. J. Appl. Meteor. Climatol. 53, 1593–1605.
- Chakrabarti, S., Bongiovanni, T., Judge, J., Zotarelli, L., Bayer, C., 2014. Assimilation of SMOS soil moisture for quantifying drought impacts on crop yield in agricultural regions. IEEE J. Selected Topics App. Earth Obs. Rem. Sens. 7 (9), 3867–3879. http://dx.doi.org/10.1109/JSTARS.2014.2315999.
- Crow, W.T., Kumar, S.V., Bolten, J.D., 2012. On the utility of land surface models for agricultural drought monitoring. Hydrol. Earth Syst. Sci. 16, 3451–3460. http://dx.doi.org/10.5194/hess-16-3451-2012.
- Diamond, H.J., Karl, T.R., Palecki, M., Baker, C.B., Bell, J.E., Leeper, R.D., Easterling, D. R., Lawrimore, J.H., Meyers, T.O., Helfert, M.R., Goodge, G., Thorne, P.W., 2013. U. S. climate reference network after one decade of operations: status and assessment. Bull. Am. Meteor. Soc. 94 (4), 489–498. http://dx.doi.org/10.1175/BAMS-D-12-00170.1.
- Draper, C.S., Mahfouf, J.F., Walker, J.P., 2009. An EKF assimilation of AMSR-E soil moisture into the ISBA land surface scheme. J. Geophys. Res. 114, D20104. http://dx.doi.org/10.1029/2008|D011650.
- Drusch, M., Wood, E.F., Gao, H., 2005. Observation operators for the direct assimilation of TRMM microwave imager retrieves soil moisture. Geophys. Res. Lett. 32, L15403. http://dx.doi.org/10.1029/2005GL023623.
- Entekhabi, D. et al., 2010a. The Soil Moisture Active Passive (SMAP) Mission. Proc. IEEE 98 (5), 704–716. http://dx.doi.org/10.1109/JPROC.2010.2043918.
- Entekhabi, D., Das, N., Njoku, E.G., Jackson, T.J., Shi, J.C., 2015. SMAP L3 radar/radiometer global daily 9 km EASE-grid soil moisture, Version 2.
- Entekhabi, D., Reichle, R.H., Koster, R.D., Crow, W.T., 2010b. Performance metrics for soil moisture retrievals and application requirements. J. Hydrometeorol. 11, 832–840. http://dx.doi.org/10.1175/2010JHM1223.1.
- FAO/IIASA/ISRIC/ISS-CAS/JRC, 2009. Harmonized World Soil Database (version 1.1). FAO, Rome, Italy and IIASA, Laxenburg, Austria.
- Fascetti, F., Pierdicca, N., Pulvirenti, L., Crapolicchio, R., Munoz-Sabater, J., 2016. A comparison of ASCAT and SMOS soil moisture retrievals over Europe and Northern Africa from 2010 to 2013. Int. J. Appl. Earth Obs. Geoin. 45, 135–142. doi: 10.1016/j.jag.2015.09.008.
- Gan, Y., Duan, Q., Gong, W., Tong, C., Sun, Y., Chu, W., Ye, A., Miao, C., Di, Z., 2014. A comprehensive evaluation of various sensitivity analysis methods: A case study with a hydrological model. Env. Model. Soft. 51, 269–285.
- Hao, Z., AghaKouchak, A., 2013. A non-parametric multivariate multi-index drought monitoring framework. J. Hydromet. 15, 89–101. http://dx.doi.org/10.1175/ IHM-D-12-0160.1
- Hunt, E.D., Hubbard, K.G., Wihite, D.A., Arkebauer, T.J., Dutcher, A.L., 2009. The development and evaluation of a soil moisture index. Int. J. Climatol. 29 (5), 747–759. http://dx.doi.org/10.1002/joc.1749.
- Jackson, T. J., Colliander, A., Kimball, J.S., Reichle, R.H., Crow, W.T., Entekhabi, D., O'Neill, P.E., Njoku, E.G., 2012. Soil Moisture Active Passive (SMAP) mission science data calibration and validation plan, pp. 1–96.
- Jackson, T., O'Neill, P., Njoku, E., Chan, S., Bindlish, R., Colliander, A., Chen, F., Burgin, M., Dunbar, S., Piepmeier, J., Cosh, M., Caldwell, T., Walker, J., Wu, X., Berg, A., Rowlandson, T., Pacheco, A., McNairn, H., Thibeault, M., Martínez-Fernández, J., González-Zamora, Á., Seyfried, M., Bosch, D., Starks, P., Goodrich, D., Prueger, J., Su, Z., van der Velde, R., Asanuma, J., Palecki, M., Small, E., Zreda, M., Calvet, J., Crow, W., Kerr, Y., Yueh, S., Entekhabi, D., 2016. Calibration and Validation for the L2/3_SM_P Version 3 Data Products, SMAP Project, JPL D-93720. Jet Propulsion Laboratory. Pasadena. CA.
- Karl, T.K., 1986. The sensitivity of the Palmer drought severity index and Palmer's Z-index to their calibration coefficients including potential evapotranspiration. J. Clim. Appl. Meteorol. 25, 77–86.
- Karl, T.R., Koscielny, A.J., 1982. Drought in the United States: 1895–1981. Int. J. Climatol. 2, 313–329.
- Kerr, Y. et al., 2010. The SMOS mission: new tool for monitoring key elements of the global water cycle. Proc. IEEE 98, 666–687. http://dx.doi.org/10.1109/ JPROC.2010.2043032.
- Koppen, W., 1900. Versuch einer Klassifikation der Klimate, vorzugsweise nach ihren Beziehungen zur Pflanzenwelt. Geographische Zeitschrift 6 (593–611), 657–679
- Koster, R.D., Guo, Z., Yang, R., Dirmeyer, P.A., Mitchel, K., Puma, M.J., 2009. On the nature of soil moisture in land surface models. J. Clim. 22, 4322–4335. http://dx. doi.org/10.1175/2009/CLI2832.1 215.
- Kumar, S.V., Reichle, R.H., Harrison, K.W., Peters-Lidard, C.D., Yatheendradas, S., Santanello, J.A., 2012. A comparison of methods for a priori bias correction in soil moisture data assimilation. Water Resour. Res. 48, W03515. http://dx.doi. org/10.1029/2010WR010261.
- Lee, J.H., Im, J., 2015. A novel bias correction method for soil moisture and ocean salinity (SMOS) soil moisture: retrieval ensembles. Remote Sens. 7, 16045– 16061. http://dx.doi.org/10.3390/rs71215824.
- Liu, Y.Y., Parinussa, R.M., Dorigo, W.A., De Jeu, R.A.M., Wagner, W., van Dijk, A.I.J.M., McCabe1, M.F., Evans, J.P., 2011. Developing an improved soil moisture dataset by blending passive and active microwave satellite-based retrievals. Hydrol. Earth Sys. Sci. 15, 425–436. http://dx.doi.org/10.5194/hess-15-425-2011.
- Martínez-Fernández, J., Gonzalez-Zamora, A., Sanchez, N., Gumuzzio, A., 2015. A soil water based index as a suitable agricultural drought indicator. J. Hydrol. 522, 265–273. http://dx.doi.org/10.1016/j.jhydrol.2014.12.051.
- Martínez-Fernández, J., Gonzalez-Zamora, A., Sanchez, N., Gumuzzio, A., Herrero-Jimenez, C.M., 2016. Satellite soil moisture for agricultural drought monitoring:

- Assessment of the SMOS derived Soil Water Deficit Index. Remote Sens. Environ. 177, 277–286. http://dx.doi.org/10.1016/j.rse.2016.02.064.
- McNairn, H. et al., 2015. The Soil Moisture Active Passive Validation Experiment 2012 (SMAPVEX12): Prelaunch Calibration and Validation of the SMAP Soil Moisture Algorithms. IEEE Trans. Geophys. Rem. Sens. 53 (5), 2784–2801. http://dx.doi.org/10.1109/TGRS.2014.2364913.
- Miralles, D.G., Crow, W.T., Cosh, M.H., 2010. Estimating spatial sampling errors in coarse-scale soil moisture estimates derived from point-scale observations. J. Hydrometeorol. 11, 1423–1429. http://dx.doi.org/10.1175/2010JHM1285.1.
- Mishra, A.K., Singh, V.P., 2010. A review of drought concepts. J. Hydrol. 391 (1–2), 202–216. http://dx.doi.org/10.1016/j.jhydrol.2010.07.012.
- Mishra, A.K., Ines, A.V.M., Das, N.N., Khedun, C.P., Singh, V.P., Sivakumar, B., Hansen, J.W., 2015. Anatomy of a local-scale drought: application of assimilated remote sensing products, crop model, and statistical methods to an agricultural drought study. J. Hydrol. 526, 15–29. http://dx.doi.org/10.1016/j.jhydrol.2014.10.038.
- O'Neill et al., 2016. Evaluation of the validated soil moisture product from the SMAP radiometer. IEEE Geosci. and Remote Sens. Sym. (IGARSS). http://dx.doi.org/10.1109/IGARSS.2016.7729023.
- O'Neill, P., Chan, S., Njoku, E., Jackson, T., Bindlish, R., Algorithm Theoretical Basis Document Level 2 & 3 Soil Moisture (Passive) Data Products. 2015.
- Pan, M., Sahoo, A.K., Wood, E.F., 2014. Improving soil moisture retrievals from a physically-based radiative transfer model. Remote Sens. Environ. 140, 130–140.
- Pan, M., Cai, X., Channey, N.W., Entekhabi, D., Wood, E.F., 2016. An initial assessment of SMAP soil moisture retrievals using high-resolution model simulations and in situ observations. Geo. Phys. Lett. 43. http://dx.doi.org/10.1002/2016GL069964.
- Parrens, M., Zakharova, E., Lafont, S., Calvet, J.C., Kerr, Y., Wagner, W., Wigneron, J.P., 2012. Comparing soil moisture retrievals from SMOS and ASCAT over France. Hydrol. Earth Syst. Sci. 16, 423–440. http://dx.doi.org/10.5194/hess-16-423-2012.
- Pribyl, D.W., 2010. A critical review of the conventional SOC to SOM conversion factor. Geoderma 156 (3–4), 75–83.
- Purcell, L.C., Sinclair, T.R., McNew, R.W., 2003. Drought avoidance assessment for summer annual crops using long-term weather data. Agron. J. 95, 1566–1576. http://dx.doi.org/10.2134/agronj2003.1566.
- Qin, W., Chi, B., Oenema, O., 2013. Long-term monitoring of rainfed wheat yield and water at the Loess Plateau reveals low water use efficiency. PLOS One 8 (11), 1–10.
- Rawls, W.J., Brakensiek, D.L., Saxton, K.E., 1982. Estimation of Soil Water Properties. Trans. ASAE 25 (5), 1316–1320.
- Reichle, R.H., Koster, R.D., 2004. Bias reduction in short records of satellite soil moisture. Geophys. Res. Let. 31 (L19501), 1–4. http://dx.doi.org/10.1029/ 2004G1020938
- Rozante, J.R., Moreira, D.S., de Goncalves, L.G., Vila, D.A., 2010. Combining TRMM and surface observations of precipitation: technique and validation over South America. Wea. Forecasting 25, 885–894. http://dx.doi.org/10.1175/2010WAF2222325.1.
- Rubel, F., Kottek, M., 2010. Observed and projected climate shifts 1901–2100 depicted by world maps of the Koppen-Geiger climate classification. Meteorologische Zeitschrif 19 (2), 135–141.
- Saxton, K.E., Rawls, W.J., 2006. Soil Water characteristics estimates by texture and organimc matter for hydrologic solution. Soil Sci. Soc. Am. J. 70, 1569–1578.
- Saxton, K.E., Rawls, W.J., Romberger, J.S., Papendick, R.I., 1986. Estimating generalized soil water characteristics from texture. Trans. ASAE 50, 1031–1035.
- Scaini, A., Sanchez, N., Vicente Serrano, S.M., Martinez-Fernandez, J., 2015. SMOSderived soil moisture anomalies and drought indices: a comparative analysis

- using in situ measurements. Hydrol. Proc. 29 (3), 373–383. http://dx.doi.org/10.1002/hyp.10150.
- Shangguan, W., Dai, Y., Duan, Q., Liu, B., Yuan, H., 2014. A global soil data set for earth system modeling. J. Adv. Model. Earth Syst. 6, 249–263. http://dx.doi.org/10.1002/2013MS000293.
- Sheffield, J., Wood, E.F., 2008. Global trends and variability in soil moisture and drought characteristics, 1950–2000, from observation-driven simulations of the terrestrial hydrologic cycle. J. Clim. 21, 432–458. http://dx.doi.org/10.1175/ 2007[CIJ1822.1.
- Shellito, P.J. et al., ellito et al. 2016. SMAP soil moisture drying more rapid than observed in situ following rainfall events. Geophys. Res. Lett. 43, 8068–8075. http://dx.doi.org/10.1002/2016GL069946.
- Soule, P.T., 1992. Spatial patterns of drought frequency and duration in the contiguous USA based on multiple drought event definitions. Int. J. Climatol. 12, 11–24. http://dx.doi.org/10.1002/joc.3370120103.
- Thornthwaite, C.W., 1948. An approach towards a rational classification of climate. Geogr. Rev. 38, 55–94.
- Torres, G.M., Lollato, R.P., Ochsner, T.E., 2013. Comparison of drought probability assessments based on atmospheric water deficit and soil water deficit. Agron. J. 105 (2), 428–436. http://dx.doi.org/10.2134/agronj2012.0295.
- Van der Schrier, G., Jones, P.D., Briffa, K.R., 2011. The sensitivity of the PDSI to the Thornthwaite and Penman-Monteith parameterizations for potential evapotranspiration. J. Geophys. Res. 116, D03106. http://dx.doi.org/10.1029/2010ID015001.
- van Genuchten, M.Th., 1980. A closed-form equation for predicting the hydraulic conductivity of unsaturated soils. Soil Sci. Soc. Am. J. 44, 892–898.
- Velpuri, N.M., Senay, G.B., Morisette, J., 2016. Evaluating new SMAP soil moisture for drought monitoring in the rangelands of the US high plains. Range Lands 38 (4), 183–190. http://dx.doi.org/10.1016/j.rala.2016.06.002.
- Vicente-Serrano, S.M., Begueria, S., Lopez-Moreno, J.I., Angulo, M., El Kenawy, A., 2010. A new global 0.5 degrees gridded dataset (1901–2006) of a multiscalar drought index: Comparison with current drought index datasets based on the Palmer Drought Severity Index. J. Hydrometeorol. 11, 1033–1043. http://dx.doi.org/10.1175/2010JHM1224.1.
- Vu, M.T., Raghavan, V.S., Liong, S.Y., 2012. SWAT use of gridded observations for simulating runoff – A Vietnam river basin study. Hydrol. Earth Syst. Sci. 16, 2801–2811. doi:10.5194/hess-16-2801-2012.
- Vu, M.T., Raghavan, V.S., Pham, D.M., Liong, S.Y., 2015. Investigating drought over the central highland, Vietnam, using Regional Climate Models. J. Hydrol. 526, 265–273. http://dx.doi.org/10.1016/j.jhydrol.2014.11.006.
- Walsh, J.E., Richman, M.B., Allen, D.W., 1982. Spatial coherence of monthly precipitation in the United States. Mon. Wea. Rev. 110, 272–286.
- Wells, N., Goddard, S., Hayes, M.J., 2004. A self-calibrating Palmer Drought Severity Index. J. Clim. 17, 2335–2351. http://dx.doi.org/10.1175/1520-0442(2004) 017<2335:ASPDSI>2.0.CO;2.
- Willmott, C.J., 1981. On the validation of models. Phys. Geogr. 2, 184-194.
- Willmott, C.J., 1982. Some comments on the evaluation of model performance. Bull. Am. Meteorol. Soc. 63, 1309–1313.
- Wosten, J.H.M., Pachepsky, Y.A., Rawls, W.J., 2001. Pedotransfer functions: bridging the gap between available basic soil data and missing soil hydraulic characteristics. J. Hydrol. 251, 123–150.
- Zhuo, L., Dai, Q., Han, D., 2015. Evaluation of SMOS soil moisture retrievals over the central United States for hydro-meteorological application. Phys. Chem. Earth 83–84, 146–155. http://dx.doi.org/10.1016/j.pce.2015.06.002.